Hindawi
International Journal of Chemical Engineering
Volume 2019, Article ID 4936292, 11 pages
https://doi.org/10.1155/2019/4936292

Research Article

Ethanol Dehydration over WO_3/TiO_2 Catalysts Using Titania Derived from Sol-Gel and Solvothermal Methods

Anchale Tresatayawed,[1] Peangpit Glinrun,[2] and Bunjerd Jongsomjit[1]

[1]*Center of Excellence on Catalysis and Catalytic Reaction Engineering, Department of Chemical Engineering, Faculty of Engineering, Chulalongkorn University, Bangkok 10330, Thailand*
[2]*Department of Petrochemicals and Environmental Management, Faculty of Engineering, Pathumwan Institute of Technology, Phathumwan, Bangkok 10330, Thailand*

Correspondence should be addressed to Bunjerd Jongsomjit; bunjerd.j@chula.ac.th

Received 23 November 2018; Accepted 12 February 2019; Published 3 March 2019

Guest Editor: Masaru Watanabe

Copyright © 2019 Anchale Tresatayawed et al. This is an open access article distributed under the Creative Commons Attribution License, which permits unrestricted use, distribution, and reproduction in any medium, provided the original work is properly cited.

The present study aims to investigate the catalytic ethanol dehydration to higher value products including ethylene, diethyl ether (DEE), and acetaldehyde. The catalysts used for this reaction were WO_3/TiO_2 catalysts having W loading of 13.5 wt.%. For a comparative study, the TiO_2 supports employed were varied by two different preparation methods including the sol-gel and solvothermal-derived TiO_2 supports, denoted as TiO_2-SG and TiO_2-SV, respectively. It is obvious that the different preparation methods essentially altered the physicochemical properties of TiO_2 supports. It was found that the TiO_2-SV exhibited higher surface area and pore volume and larger amounts of acid sites than those of TiO_2-SG. As a consequence, different characteristics of support apparently affected the catalytic properties of WO_3/TiO_2 catalysts. As expected, both catalysts WO_3/TiO_2-SG and WO_3/TiO_2-SV exhibited increased ethanol conversion with increasing temperatures from 200 to 400°C. It appeared that the highest ethanol conversion (ca. 88%) at 400°C was achieved by the WO_3/TiO_2-SV catalysts due to its high acidity. It is worth noting that the presence of WO_3 onto TiO_2-SV yielded a remarkable increase in DEE selectivity (ca. 68%) at 250°C. In summary, WO_3/TiO_2-SV catalyst is promising to convert ethanol into ethylene and DEE, having the highest ethylene yield of ca. 77% at 400°C and highest DEE yield of ca. 26% at 250°C. These can be attributed to proper pore structure, acidity, and distribution of WO_3.

1. Introduction

Recently, catalytic ethanol dehydration to produce ethylene and diethyl ether (DEE) has been paid attention due to its cleaner technology and efficient utilization of ethanol, which is a renewable raw material obtained from fermentation of biomass. For instance, the production of ethylene from ethanol is considered as an alternative way to produce ethylene, which is currently produced by the catalytic thermal cracking of petroleum feed stocks such as naphtha and dehydrogenation of ethane from natural gas. In fact, dehydration of ethanol to ethylene is a cleaner technology due to lower operating temperature, uncomplicated process, and less impurity. It is well known that ethylene is one of the most important raw materials for petrochemical industry, which is used as a starting material for production of polyethylene, ethylene oxide, vinyl acetate, ethyl benzene, etc. Considering the production of commercialized DEE at present, although it is produced from dehydration of ethanol, the process is not benign since it uses mineral liquid acids such as H_2SO_4 to catalyze the reaction. Thus, further separation and purification are required. In this case, the solid acid catalysts are preferred since they are reusable and easy to separate from the product. Although the use of DEE is much lesser than ethylene, it is very important chemical. In particular, DEE is mainly employed as a solvent for fragrance and pharmaceutical industries. In transport fuel function, DEE is applied as an ignition-improving additive in engines according to its high volatility and cetane and octane number. The blending of DEE in diesel improves the

performance-emission characteristics with thermal efficiency and reduced emission of NOx, CO, and HC [1]. Hence, the production of ethylene and DEE from ethanol using suitable solid catalysts is very captivating.

Theoretically, the catalytic ethanol dehydration to ethylene and DEE requires acid sites. This reaction essentially undergoes via thermodynamic and kinetic controls. The formation of ethylene is dominated by high reaction temperature since it is an endothermic reaction, whereas DEE mainly occurs at lower reaction temperature due to its exothermic reaction. However, during dehydration of ethanol, a side reaction such as dehydrogenation can occur resulting in the formation of acetaldehyde as a byproduct. From previous works, many solid acid catalysts have been investigated in ethanol dehydration reaction including the transition metal oxides [2–4], zeolites [5], silica-alumina [6, 7], and heteropolyacids [8]. Many researchers found that the transition metal oxides such as TiO_2, ZrO_2, SiO_2, and Nb_2O_5 play an important role in heterogeneous catalysis acting as an active phase, promoter, or support of solid catalysts. Those solid catalysts have been developed on structure characteristics and acid properties to build up the product selectivity, catalytic activity, and stability. Among the transition metal oxides, TiO_2 has been widely used as a support in heterogeneous catalysts due to its suitable surface areas, thermal stability and mechanical resistance [9, 10]. Furthermore, the modification by doping of the active noble and transition metals such as Cs [11], Au/Ag/Cu [12], Al [13], Ru [14], Pt, Pd [15], Mo [16], and W [17, 18] into catalyst supports apparently affected the catalyst selectivity and activity.

In addition, the presence of tungsten (W) metal was found to be very interesting since it contributes Brønsted acid site and increases the catalyst stability and activity [19–21]. It is reported that WO_3/TiO_2 catalyst is widely used in various reactions and processes including glycerol hydrogenation, reforming, oxidation of dibenzothiophene [22], selective catalytic reduction [23], dehydration [24], and photoelectrocatalytic degradation [25]. Phung et al. [26] also reported that WO_3/TiO_2 is promising for the catalytic dehydration of ethanol to ethylene and especially DEE at low temperature. They reported that the addition of tungsten on transition metal oxide provided the Brønsted acids sites that are active to the ethanol dehydration reaction to produce ethylene and DEE and also prevent the formation of byproducts such as acetaldehyde and higher hydrocarbons. In addition, with various tungsten loadings on TiO_2, ZrO_2 and SiO_2 support, the WO_3/TiO_2 catalyst was found to be the most active in this reaction giving the highest yield of DEE. However, besides the active metals, one needs to consider on the properties of a wide variety of supports themselves. The variations of support characteristics mostly arise from different preparation methods. There are many reports focusing on using different methods to prepare various metal oxide supports including the sol-gel [27, 28] and solvothermal methods [29, 30]. In most cases, they found that different preparation methods can alter the properties of support and consequently, different catalytic properties were observed. Therefore, the effect of different preparation methods on the properties of support is crucial for better understanding.

Similarly to Phung et al. [26] study, the WO_3/TiO_2 catalyst was employed in ethanol dehydration reaction. They examined the difference in some support metal oxides such as ZrO_2 and SiO_2. However, the main goal of this present study is to develop a better understanding on different preparation methods including the sol-gel and solvothermal methods to synthesize the TiO_2 supports for WO_3 catalysts used in catalytic ethanol dehydration to ethylene and DEE. The different characteristics of TiO_2 supports and WO_3/TiO_2 catalysts were determined using various characterization techniques. The change in catalytic properties was also investigated via the catalytic ethanol dehydration in a fixed-bed microreactor at the temperature range of 200 to 400°C. Ethanol conversion and product selectivity of different WO_3/TiO_2 catalysts were reported and discussed further.

2. Experimental

2.1. Materials. Chemicals used for preparation of the catalysts were titanium ethoxide (Ti ~ 20%) purchased from Aldrich, ethanol (99.99%) from Merck Company Ltd., titanium (IV) *n*-butoxide (97%), 1,4–butanediol, and tungsten (VI) chloride (99.9+% metals) from Aldrich. For the reaction study, ultrahigh purity nitrogen gas (99.99%) from Linde (Thailand) Public Company Ltd. was employed.

2.2. Preparation of TiO_2 Supports and WO_3/TiO_2 Catalysts. In this study, TiO_2 supports were synthesized using two different methods including the sol-gel and solvothermal methods as reported by Panpranot et al. [29] for a comparative study. For the sol-gel method, titanium ethoxide was used as the precursor. First, the precursor was dissolved in the excess ethanol before added to deionized water with the molar ratio of 165. The mixture solution was stirred under 20 rpm/min at room temperature at least for 2 h. The white precipitates of hydrous oxides formed instantly and separated by centrifugation. The product was redispersed in the ethanol at least 5 times following with centrifugation. The sample was dried and calcined at 450°C for 2 h at the heating rate of 10°C/min. Finally, the white powder of TiO_2 prepared by the sol-gel method was obtained and denoted as TiO_2-SG.

For the solvothermal method, 25 g of titanium (IV) *n*-butoxide (TNB) was used as the precursor. TNB was suspended in 100 ml of 1,4-butanediol in a test tube and placed in the autoclave. The autoclave was completely purged with nitrogen at a pressure of 30 bars before increasing the temperature to 320°C at a heating rate of 2.5°C/min and further held at that temperature for 6 h. Autogenous pressure during the reaction gradually increased as the temperature increased. After the reaction, the autoclave was cooled down to room temperature. The white powder was collected and then washed with ethanol followed by centrifugation at least 5 times. The powder was dried overnight at 110°C, and finally the white powder of TiO_2 prepared

by the solvothermal method was obtained and denoted as TiO_2-SV.

In order to prepare the WO_3/TiO_2 catalysts having W loading of 13.5 wt.%, the simple incipient wetness impregnation was used. The TiO_2-SG and TiO_2-SV supports obtained as mentioned above were used. It was accomplished using the tungsten (VI) chloride as a precursor, followed by drying the catalyst sample overnight at 110°C and calcined at 400°C with a heating rate of 10°C/min for 3 h. Consequently, the obtained WO_3/TiO_2 catalysts are denoted as WO_3/TiO_2-SG and WO_3/TiO_2-SV upon the TiO_2 supports employed.

2.3. Catalysts Characterization. The support and catalysts were characterized by several techniques, which are as follows.

2.3.1. Powder X-Ray Diffraction (XRD). The SIEMENS D-5000 X-ray diffractometer using CuK_α radiation ($\lambda = 1.54439$ Å) was used to determine the crystalline phase structure of supports and catalysts. The crystalline domain sizes were calculated from the Scherrer equation. The supports and catalysts were scanned at a rate of 2.4 min^{-1} in the range 2θ from 20 to 80 degrees with the resolution of 0.02°.

2.3.2. N_2 Physisorption. The adsorptiometer Micromeritics ASAP 2010 automated system instrument was used to determine surface area (BET method), pore volume/diameter, and pore size distribution (BJH method) by nitrogen gas adsorption-desorption at liquid nitrogen temperature at −196°C.

2.3.3. Temperature-Programmed Desorption of Ammonia (NH_3-TPD) and Carbon Dioxide (CO_2-TPD). The Micromeritics Chemisorb 2750 Pulse chemisorption system instrument was employed to identify the acidity and basicity on supports and catalysts. The 0.03 g quartz wool and 0.05 g catalysts were packed in a quartz tube and pretreated at 500°C under He flow for 1 hr. Next, the catalyst surface was saturated with NH_3 or CO_2 in He at 40°C for 30 min. Then, the excess adsorbed gas (the physisorbed NH_3 or CO_2) was purged with He until the baseline was constant. Afterwards, the catalysts was heated from 40°C to 500°C at a heating rate of 10°C/min to desorb NH_3 or CO_2. The amount of NH_3 or CO_2 in effluent was measured via the thermal conductivity detector (TCD) signal as a function of temperature.

2.3.4. Scanning Electron Microscopy (SEM) and Energy Dispersive X-Ray Spectroscopy (EDX). The SEM model JEOL mode JSM-6400 and EDX with stand Link Isis series 300 program were operated for analysis the morphology, element composition, and distributions over supports and catalysts.

2.3.5. X-Ray Fluorescence Analysis (XRF). The Olympus model Vanta M Series was performed to determine the amount of tungsten loading on catalysts. XRF spectrometer has an X-ray tube with Rh anode. The spectra were collected during 120 s, with the tube operating with a current of 100 μA and a voltage of 40 kV.

2.3.6. Catalytic Ethanol Dehydration Reaction. Essentially, the ethanol dehydration reaction system reported by Krutpijit and Jongsomjit was used [31]. It was performed in a fixed-bed continuous flow microreactor having an inside diameter of 0.7 cm and length of 33 cm length. First, 0.01 g of quartz wool and 0.05 g of catalyst (or support) were packed in the middle of reactor. The catalyst was preheated by flowing N_2 with a flow rate of 60 ml/min at 200°C for 1 h under atmospheric pressure to remove the moisture and impurity on surface of catalyst prior reaction. Afterwards, the reaction was started by feeding vaporized ethanol and N_2 stream as carrier gas. The ethanol flow rate was maintained at 1.45 ml/h (weight hourly space velocity (WHSV) = 22.9 ($g_{ethanol} \cdot g_{cat}{}^{-1} \cdot h^{-1}$)) controlled by a syringe pump injection. The reaction was operated at temperature varied from 200 to 400°C. After reaching steady-state condition, the reaction product compositions at reactor effluent were analyzed by a Shimadzu gas chromatography (GC8A) with flame ionization detector (FID) using DB-5 capillary column. Nitrogen with the pressure at 260 kPa was used as carrier gas in GC using the temperature of injector and detector at 150°C. The ethanol conversion was defined as follows:

$$X_{\mathrm{EtOH}} = \frac{n_{\mathrm{EtOH(in)}} - n_{\mathrm{EtOH(out)}}}{n_{\mathrm{EtOH(in)}}} \times 100. \quad (1)$$

The selectivity to i product was defined as follows:

$$S_{\mathrm{ethylene}} = \frac{n_{\mathrm{ethylene}}}{\sum n_i} \times 100,$$

$$S_{\mathrm{DEE}} = \frac{n_{\mathrm{DEE}}}{\sum n_i} \times 100, \quad (2)$$

$$S_{\mathrm{acetaldehyde}} = \frac{n_{\mathrm{acetaldehyde}}}{\sum n_i} \times 100.$$

The yield to i product was defined as follows:

$$Y_{\mathrm{ethylene}} = \frac{S_{\mathrm{ethylene}} \times X_{\mathrm{EtOH}}}{100},$$

$$Y_{\mathrm{DEE}} = \frac{S_{\mathrm{DEE}} \times X_{\mathrm{EtOH}}}{100}, \quad (3)$$

$$Y_{\mathrm{acetaldehyde}} = \frac{S_{\mathrm{acetaldehyde}} \times X_{\mathrm{EtOH}}}{100},$$

where $n_{\mathrm{EtOH(in)}}$ and $n_{\mathrm{EtOH(out)}}$ are defined as the molar flow rate (mmol/min) of ethanol in feed and product, respectively. n_{Ethylene}, n_{DEE}, $n_{\mathrm{Acetaldehyde}}$, and $\sum n_i$ were defined as the molar flow rate of ethylene, DEE, acetaldehyde, and total products (mmol/min), respectively.

3. Results and Discussion

3.1. Characteristics. The XRD patterns of both TiO_2 supports and WO_3/TiO_2 catalysts are illustrated in Figure 1.

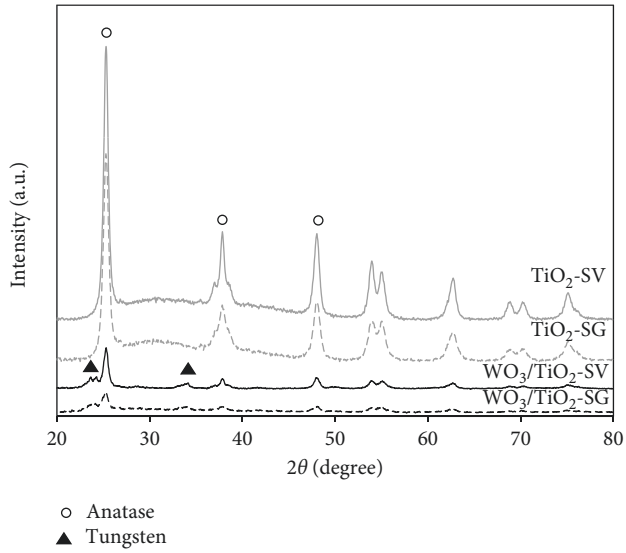

Figure 1: X-ray powder diffraction patterns of supports and catalysts.

Considering the XRD patterns of the supports including TiO_2-SG and TiO_2-SV, they exhibited the similar XRD patterns having the strong diffraction peaks located at 2θ degree of 25° (major), 38°, and 48°, which are assigned to the tetragonal anatase phase of crystalline TiO_2 [32, 33]. When the support was impregnated with 13.5 wt.% of tungsten, the XRD patterns were also similar with those of titania supports. The intensities were lower indicating the smaller crystallite size of WO_3/TiO_2 catalysts than the TiO_2 supports. Besides, the low intensity peaks were observed at 24° and 34° for both WO_3/TiO_2-SG and WO_3/TiO_2-SV catalysts, which were assigned to the formation of the WO_3 crystals with tetragonal phase [34, 35]. When compared the intensity of XRD peaks between WO_3/TiO_2-SG and WO_3/TiO_2-SV, it appeared that WO_3/TiO_2-SG exhibited lower intensity than WO_3/TiO_2-SV suggesting that the crystalline size of the former was smaller than the latter. Based on the Scherrer equation, the average crystalline size of WO_3/TiO_2-SG was smaller than WO_3/TiO_2-SV as seen in Table 1, where the TiO_2 crystalline size was in the range of 10.7–14.3 nm.

The BET surface area (S_{BET}), pore volume, and pore size diameter of TiO_2 supports and WO_3/TiO_2 catalysts analyzed by N_2 physisorption are shown in Table 1. The results revealed that the TiO_2-SG exhibited smaller surface area (73 m^2/g) and pore volume (0.13 cm^3/g) than those of TiO_2-SV BET surface area (85 m^2/g) and pore volume (0.42 cm^3/g). The large surface area essentially enhances catalytic activity in ethanol dehydration by increasing possibility of ethanol to attach on the acid site [28]. In addition, the surface area, pore volume, and pore size diameter decreased with the presence of tungsten due to some pore blockage [36].

Figure 2 showed the N_2 adsorption-desorption isotherms at −196°C for the TiO_2 supports and WO_3/TiO_2 catalysts. The results displayed the Type IV adsorption isotherms with the H1 hysteresis loop indicating the mesoporous structure according to the IUPACS. After loading tungsten to obtain WO_3/TiO_2-SG and WO_3/TiO_2-SV, it was found that the Type IV isotherm was still observed. The hysteresis loop moved toward lower pressure for WO_3/TiO_2-SG and WO_3/TiO_2-SV suggesting that the addition of tungsten onto TiO_2 support catalyst resulted in decreased pore volume. The pore size distribution (PSD) for the TiO_2 support catalysts and catalysts are shown in Figure 3. All catalysts were in the average pore diameter range of 2–50 nm classified as mesoporous particles. The TiO_2-SG showed the narrower pore size distribution than that of TiO_2-SV. The average pore sizes for all samples calculated by Barrett–Joyner–Halenda (BJH) are shown in Table 1, which were corresponding to the results from N_2 adsorption-desorption isotherm as seen from Figure 2.

The morphology of supports and catalysts prepared by different methods showed the different morphologies. The TiO_2-SG formed irregular shape particles, while TiO_2-SV formed small agglomerated spherical and porous particles. When impregnated with tungsten on TiO_2-SG and TiO_2-SV supports, both samples exhibited more porous particles. This suggested that the presence of tungsten into TiO_2 resulted in an increase of porosity. The EDX mapping of WO_3/TiO_2-SG and WO_3/TiO_2-SV catalysts are illustrated in Figure 4. It shows the elemental distribution of Ti, O, and W dispersing on the external surface of catalysts.

The tungsten was well dispersed at the outer surface of both TiO_2-SG and TiO_2-SV. The weight ratios of W/Ti are also listed in Table 2. The amount of tungsten present at outer surface of TiO_2-SG was larger than TiO_2-SV. Nevertheless, according to the XRF analysis the amount of tungsten in the bulk of TiO_2-SV catalyst was larger than TiO_2-SG indicating that the distribution of tungsten for TiO_2-SV catalyst was mostly located inside the pore of catalyst.

It is well known that acidity is the key factor relating to the activity of dehydration catalysts. The acidity of

Table 1: Physical properties of TiO_2 supports and catalysts.

Sample	S_{BET} (m^2/g)	Pore volume (cm^3/g)	Pore diameter (nm)	Crystallite TiO_2 size[a] (nm)	Crystallite WO_3 size[a] (nm)	W content[b] (wt.%)
TiO_2-SG	73	0.13	4.8	12.4	—	—
TiO_2-SV	85	0.42	16.5	15.3	—	—
WO_3/TiO_2-SG	61	0.11	5.1	10.7	6.1	16.3
WO_3/TiO_2-SV	78	0.30	13.0	14.3	9.0	18.9

[a]Measured by XRD using the Scherrer equation, [b]measured by XRF.

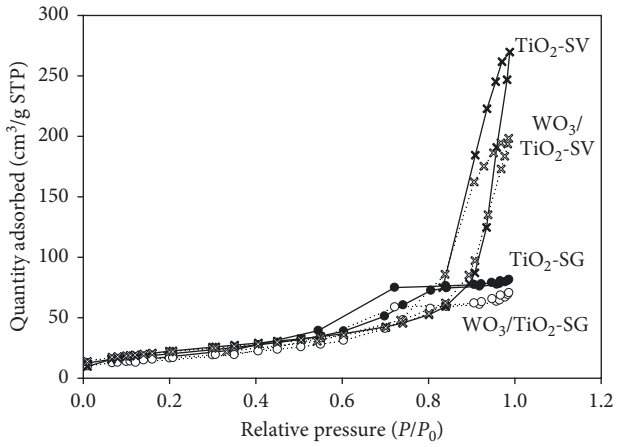

Figure 2: Nitrogen adsorption-desorption isotherms for supports and catalysts.

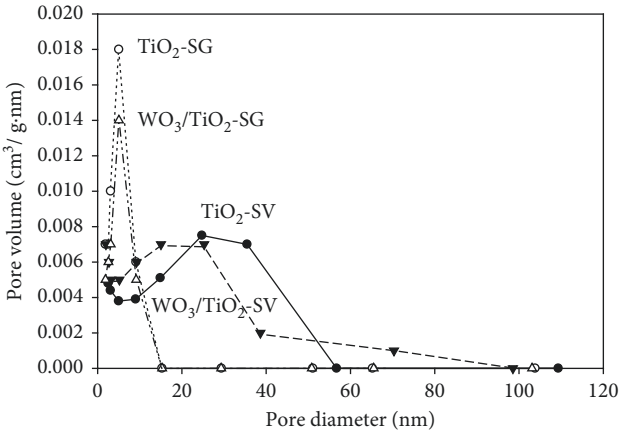

Figure 3: The pore size distribution for supports and catalysts.

supports and catalysts was evaluated by NH_3-temperature-programmed desorption as shown in Figure 5. As observed, the NH_3-TPD profiles for all samples exhibited the broad desorption peaks in range of 150–500°C.

It is known that the NH_3-TPD desorption temperature of acidic sites are classified as 3 categories. The desorption of NH_3 between 150 and 300°C is assigned as weak acidic sites, whereas the desorption between 300 and 450°C is moderate acid sites and the desorption above 450°C is strong acid sites [37]. As seen in Table 3, it indicated that the TiO_2-SG exhibited lower amount of acid site than the TiO_2-SV. However, with tungsten loading on both supports, it showed significant increase in weak and total acid sites for both WO_3/TiO_2-SG and WO_3/TiO_2-SV catalysts, which is necessary for enhancing the production of ethylene and DEE [38, 39]. In addition, it can be observed that the WO_3/TiO_2-SV catalyst exhibited the highest amount of total acid sites at 3645 μmol/g cat.

Considering the CO_2-TPD profiles as shown in Figure 6, the desorption peak displayed the narrow desorption in the temperature range of 50–200°C. Both TiO_2 supports exhibited low temperature CO_2 desorption around 87°C assigned to weak basic sites [40, 41]. The addition of tungsten into support catalysts resulted in a decrease of peak intensity around 80°C. It also revealed that WO_3/TiO_2-SG had the higher amount of basicity site than WO_3/TiO_2-SV as seen in Table 4.

The amounts of carbon deposition after reaction obtained by EDX measurement are shown in Table 5. The WO_3/TiO_2-SG and WO_3/TiO_2-SV exhibited higher amounts of carbon deposition than those of the TiO_2 supports due to their higher acidity. It is well known that high acidity yields high amount of carbon deposition.

3.2. Ethanol Dehydration Reaction. To investigate the catalytic activity and product distribution for all catalysts, the ethanol dehydration reaction in gas phase at atmospheric pressure and temperature ranging from 200°C to 400°C was performed. As seen in Table 6, the ethanol conversion for all samples increased with increasing reaction temperature indicating no deactivation of supports and catalysts. The highest ethanol conversion was achieved at 400°C for all samples. The ethanol conversion was found in order of WO_3/TiO_2-SV (87.6%) > TiO_2-SV (56.3%) > WO_3/TiO_2-SG (45.4%) > TiO_2-SG (33.9%), which are related to total amount acid sites of catalysts. It should be noted that the conversion of TiO_2-SV was still higher than that of WO_3/TiO_2-SG, which is quite interesting.

The selectivity to ethylene, DEE, and acetaldehyde are presented in Table 6. It can be observed that the TiO_2 rendered acetaldehyde as a major product. However, with the introduction of tungsten into TiO_2 supports, ethylene and DEE are turned out to be the major products at different temperature. In general, ethanol dehydration reaction can produce ethylene and DEE in 2 competitive pathways:

$$C_2H_5OH \longrightarrow C_2H_4 + H_2O + 44.9 \text{ kJ/mol} \quad (4)$$

$$2C_2H_5OH \longrightarrow C_2H_5OC_2H_5 + H_2O - 25.1 \text{ kJ/mol} \quad (5)$$

The reaction (4) is endothermic and favors the moderate to high temperature between 320°C and 500°C, while

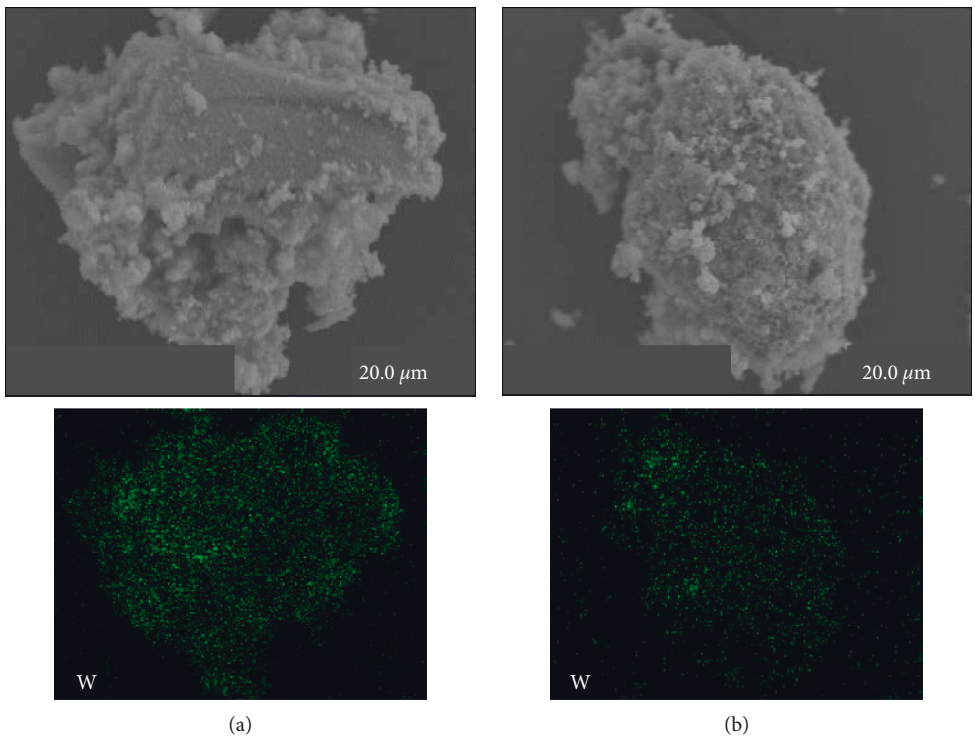

Figure 4: Elemental distribution by EDX mapping for (a) WO_3/TiO_2-SG and (b) WO_3/TiO_2-SV catalyst.

Table 2: Elemental compositions (wt.%) on external surface of catalysts obtained from EDX.

Sample	O	Ti	W	Cl	W/Ti
TiO_2-SG	44.67	55.33	n.a.	n.a.	n.a
TiO_2-SV	44.37	55.63	n.a.	n.a.	n.a
WO_3/TiO_2-SG	30.71	35.17	33.84	0.28	0.96
WO_3/TiO_2-SV	39.00	48.25	12.36	0.39	0.26

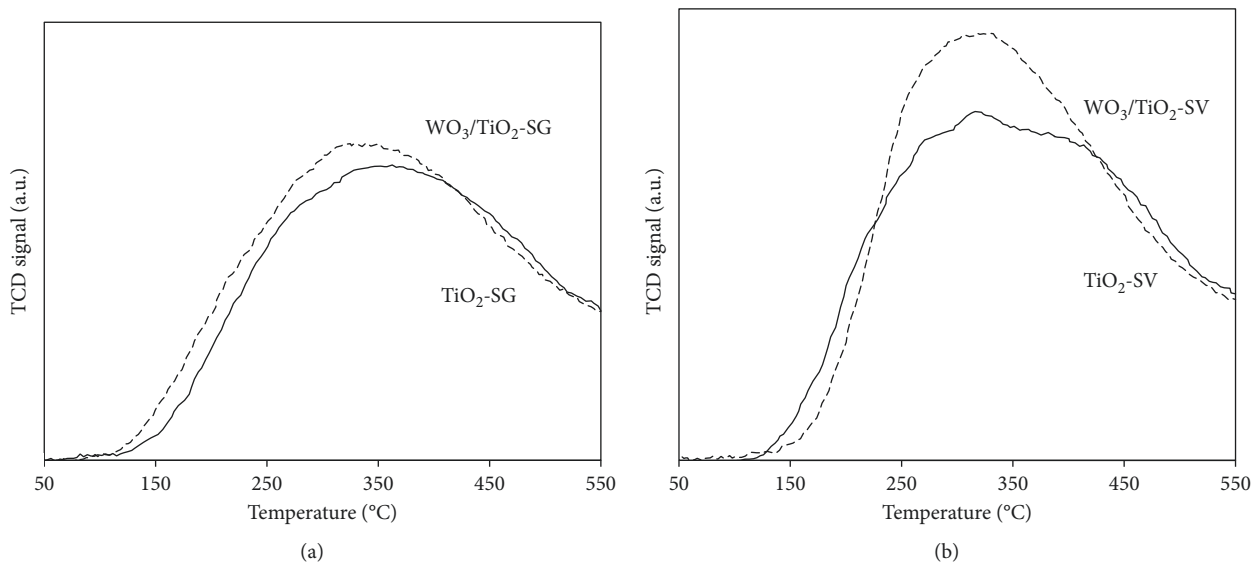

Figure 5: NH_3-TPD profiles of TiO_2 supports and WO_3/TiO_2 catalysts.

Table 3: The amount of surface acidity of supports and catalysts measured by NH_3-TPD.

Sample	NH_3 desorption (μmol/g cat)			Total acidity (μmol/g cat)
	Weak	Medium	Strong	
TiO_2-SG	895	662	717	2274
TiO_2-SV	1152	1232	841	3224
WO_3/TiO_2-SG	1030	1054	681	2765
WO_3/TiO_2-SV	1558	1263	823	3645

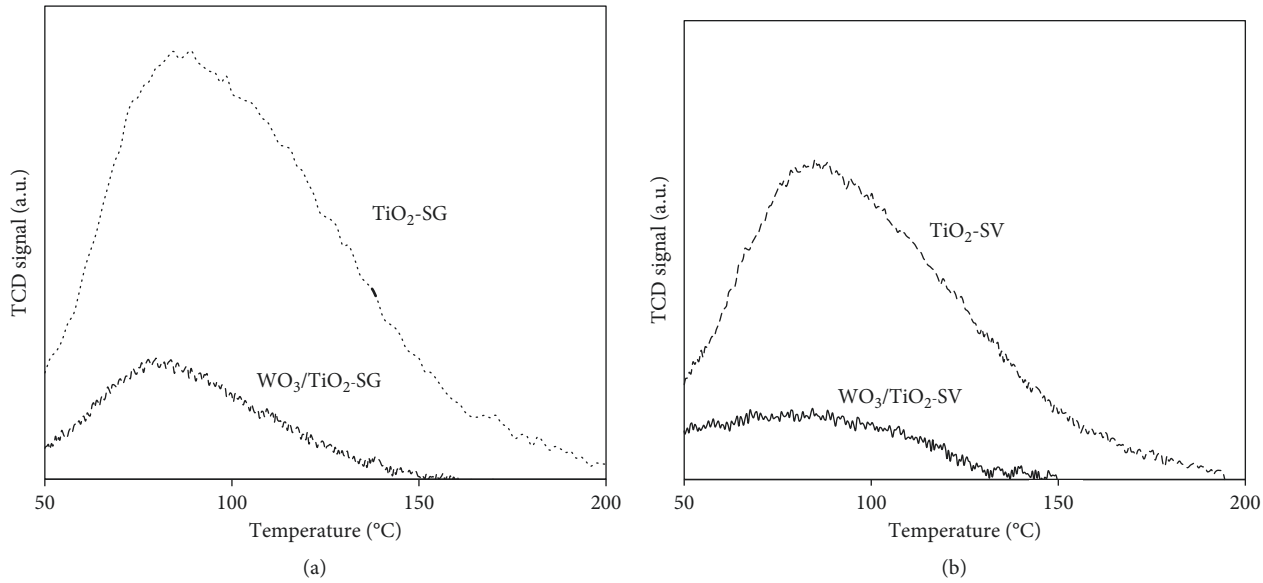

Figure 6: CO_2-TPD profile of TiO_2 supports and WO_3/TiO_2 catalysts.

Table 4: The amount of surface basicity of supports and catalysts measured by CO_2-TPD.

Sample	CO_2 desorption (μmol/g cat)		Total basicity (μmol/g cat)
	Weak	Medium/strong	
TiO_2-SG	27	4	31
TiO_2-SV	18	2	20
WO_3/TiO_2-SG	6	1	7
WO_3/TiO_2-SV	4	0	4

Table 5: The amount of carbon elemental compositions (wt.%) on external surface supports and catalysts after reaction obtained from EDX (the spent catalyst used in the reaction condition at $T = 200$–400°C for 8.5 hr).

Sample	TiO_2-SG	TiO_2-SV	WO_3/TiO_2-SG	WO_3/TiO_2-SV
C (%)	1.0	1.2	1.8	4.5

reaction (5) is exothermic and favors the low to moderate temperature between 150°C and 300°C [42]. The formation of the ethylene occurs by acid catalyst protonating to hydroxyl group of ethanol molecule (proton transfers from acid to O atom to form alkyloxonium ion), and then the water molecules is generated. Subsequently, an ethoxide surface group forms and deprotonates its methyl group to produce the ethylene. The DEE formation proceeds via either dissociative pathway or associative pathway [43]. The dissociative pathway is happened by one ethanol adsorption on catalyst and water elimination providing an adsorbed ethyl group. After that, the ethyl group reacts with the second ethanol and finally the DEE is formed. The associative pathway takes place from coadsorption of two ethanol reacted and formed into DEE. It is recognized that the dehydration of alcohol essentially takes place on Brønsted acid sites [39, 44], while Lewis acid sites rarely contribute for this reaction [45, 46]. The mechanism of ethanol dehydration to ethylene and DEE over the WO_3/TiO_2 catalysts is illustrated in Schemes 1 and 2, respectively. Besides, acetaldehyde is produced under the side reaction or dehydrogenation reaction in reaction (6), which is favored on the basic sites:

$$C_2H_5OH \longrightarrow C_2H_4O + H_2 + 52.4 \text{ kJ/mol} \quad (6)$$

According to the experiment, it was observed that TiO_2-SG and TiO_2-SV support catalysts still showed high acetaldehyde selectivity at ca. 81°C and ca. 71°C, respectively. This is perhaps due to the high reaction temperature or the heat treatment effect to an oxidation of Lewis oxygen in pure TiO_2 structure with the basic site is more dominant than acid as seen from the pure SBA-15 catalyst used in ethanol dehydration reported by Autthanit and Jongsomjit in 2018 [47]. The mechanism of ethanol dehydrogenation to acetaldehyde over TiO_2 support is illustrated in Scheme 3. Acetaldehyde occurs by ethanol molecule firstly adsorbed on the catalyst surface. An

Table 6: Ethanol conversion, product selectivity, and product yield as a function of reaction temperature (the reaction condition: $T = 200–400^{\circ}C$, WHSV = 22.9 $g_{ethanol} \cdot g_{cat}^{-1} \cdot h^{-1}$, and catalyst weight = 0.05 (g)).

Catalyst	Temp (°C)	Ethanol conversion (%)	Product selectivity (%)			Product yield (%)		
			Ethylene	DEE	Acetaldehyde	Ethylene	DEE	Acetaldehyde
TIO_2-SG	200	4.5	0.0	0.0	100.0	0.0	0.0	4.5
	250	8.6	1.8	0.0	98.2	0.2	0.0	8.5
	300	13.2	4.0	2.6	93.4	0.5	0.3	12.3
	350	32.3	11.4	1.6	87.0	3.7	0.5	28.1
	400	33.9	17.7	0.9	81.4	6.0	0.3	27.6
TIO_2-SV	200	21.1	0.0	0.0	100.0	0.0	0.0	21.1
	250	23.2	0.0	0.0	100.0	0.0	0.0	23.2
	300	35.7	2.5	2.1	95.3	0.9	0.8	34.1
	350	54.3	9.7	2.4	87.8	5.3	1.3	47.7
	400	56.3	25.5	3.4	71.1	14.4	1.9	40.0
WO_3/TiO_2-SG	200	12.4	4.7	37.4	57.9	0.6	4.6	7.2
	250	16.4	17.1	40.9	42.0	2.8	6.7	6.9
	300	25.0	39.5	10.4	50.1	9.9	2.6	12.5
	350	33.4	54.5	3.3	42.3	18.2	1.1	14.1
	400	45.4	64.6	1.3	34.1	29.3	0.6	15.5
WO_3/TiO_2-SV	200	33.2	5.2	42.6	52.2	1.7	14.2	17.3
	250	37.7	22.4	67.7	10.0	8.4	25.5	3.8
	300	51.8	52.6	42.4	5.0	27.3	22.0	2.6
	350	71.7	76.4	17.8	5.8	54.8	12.8	4.1
	400	87.6	88.2	3.5	8.3	77.2	3.1	7.3

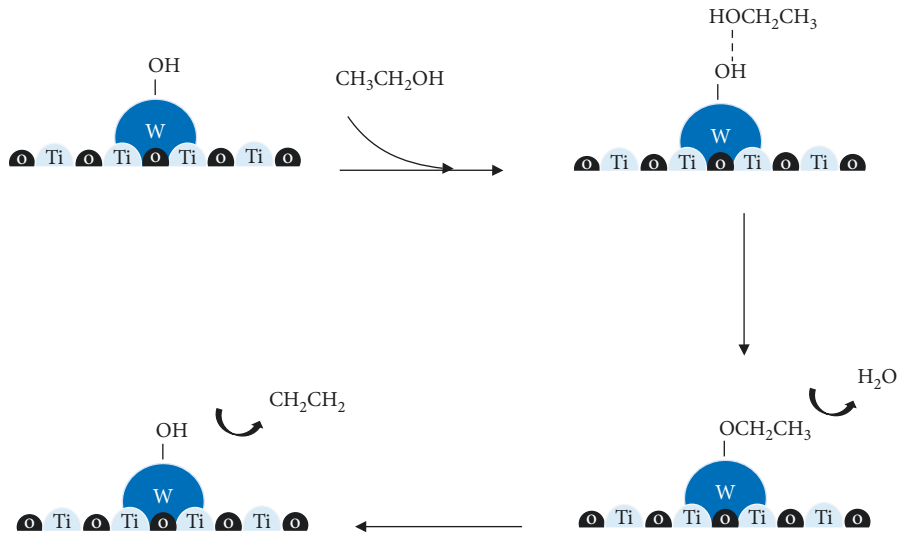

Scheme 1: Ethanol dehydration to ethylene over WO_3/TiO_2 catalyst.

ethoxy group is further generated and converted into acetaldehyde. When impregnated the tungsten on the TiO_2 supports, it revealed increased ethylene selectivity at high temperature and increased DEE selectivity at low temperature. The ethylene and DEE selectivities over WO_3/TiO_2-SV catalyst were higher than those of WO_3/TiO_2-SG catalyst. It was found that the highest ethylene selectivity of ca. 88% under the reaction temperature at 400°C and the highest DEE selectivity of ca. 68% under the reaction temperature at 250°C for WO_3/TiO_2-SV. The factor to increase the ethylene and DEE selectivity is the high amount of weak acid or Brønsted acid, which is the active site for ethanol dehydration after adding the tungsten on TiO_2 supports. As shown in Table 3, the weak acid sites for WO_3/TiO_2 catalyst were significantly higher than TiO_2 support catalyst, whereas the strong acid sites for TiO_2 were higher than the WO_3/TiO_2 catalyst. It is familiar that amount of weak acid site is probably correlated to Brønsted acid site, while the Lewis acid site may correlate to the strong acid site [47].

Besides two products, the acetaldehyde was formed as byproduct over WO_3/TiO_2-SG and WO_3/TiO_2-SV catalysts.

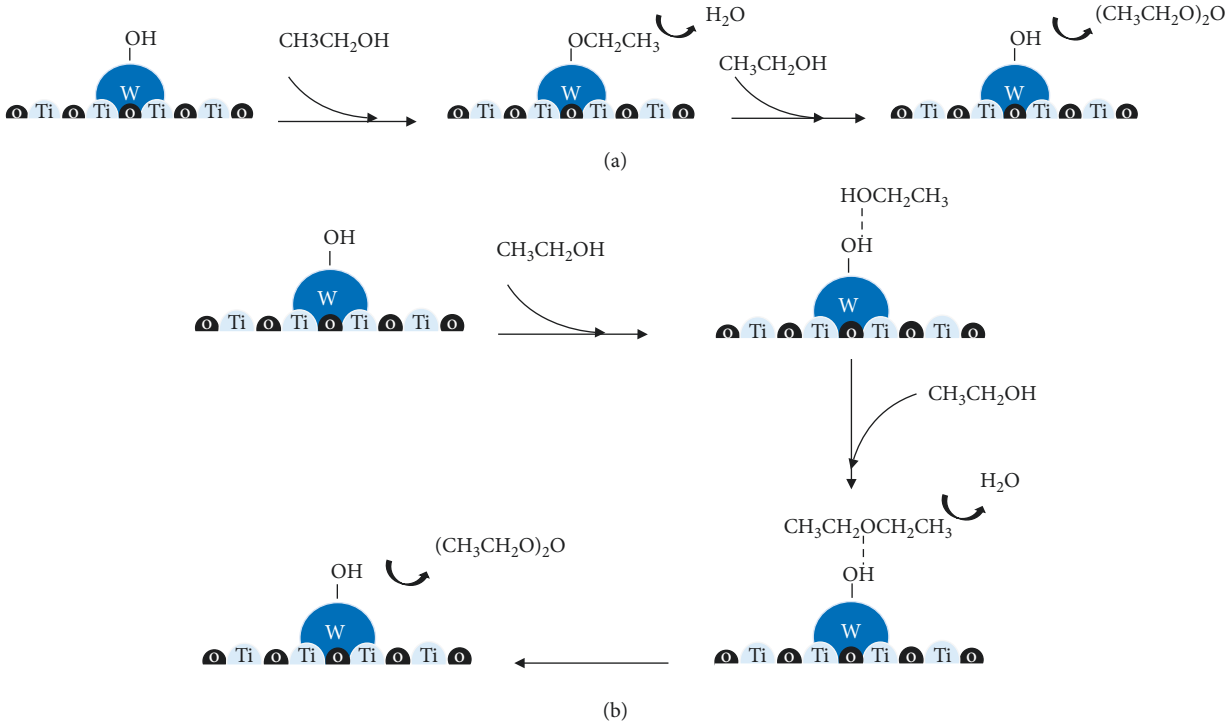

Scheme 2: Ethanol dehydration to DEE with (a) dissociative and (b) associative pathways over WO_3/TiO_2 catalyst.

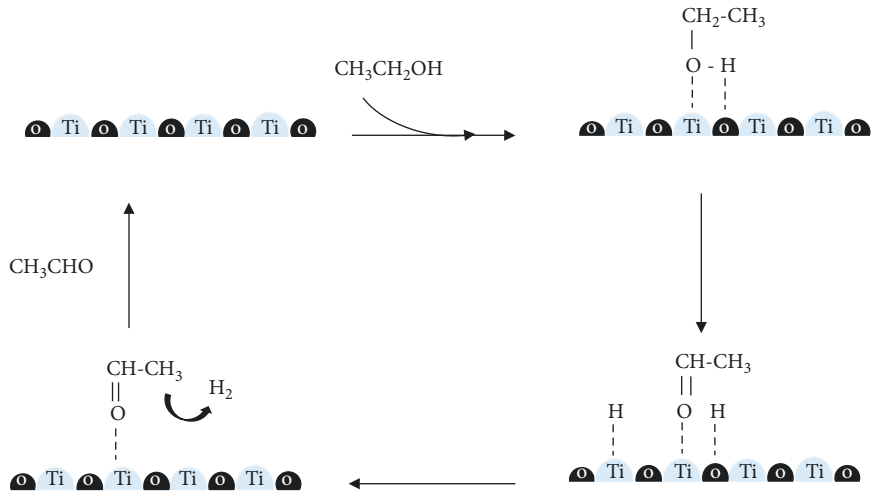

Scheme 3: Ethanol dehydrogenation to acetaldehyde over TiO2 support catalyst.

The acetaldehyde selectivity over WO_3/TiO_2-SG was higher than that of WO_3/TiO_2-SV relating to higher amounts of basic site present in WO_3/TiO_2-SG catalyst. The mass balance (carbon balance) in the reaction test typically closed to 90%. Such a deviation may occur due to mainly from coke formation.

The comparison of product yield for each temperature over supports and catalysts is reported in Table 6. It showed that presence of tungsten essentially improved the ethylene and DEE yield. The highest ethylene yield was found to be ca. 77% at 400°C over WO_3/TiO_2-SV. Moreover, it was observed that the highest DEE yield of ca. 26% at 250°C was obtained with WO_3/TiO_2-SV. However, DEE yield was rather small due to the low conversion at low temperature. It should be mentioned that the highest acetaldehyde yield of ca. 48% at 350°C obtained from TiO_2-SV was observed, which is quite interesting.

4. Conclusion

The WO_3/TiO_2-SV catalyst is promising for dehydration of ethanol to ethylene and DEE having the highest ethylene of 77% at 400°C and the highest yield of 26% at 250°C. It showed that the more efficient method to synthesize TiO_2

support was the solvothermal method due to high acidity and surface area. It is worth noting that the TiO_2-SV itself also rendered the highest yield of acetaldehyde at 48% at 350°C. This support can be potentially used as support for a catalyst in dehydrogenation of ethanol to acetaldehyde.

Data Availability

The data used to support the findings of this study are included within the article.

Conflicts of Interest

The authors declare that there are no conflicts of interest regarding the publication of this paper.

Acknowledgments

The authors thank the Grant for International Research Integration: Chula Research Scholar, Ratchadaphiseksomphot Endowment Fund, Endowment Fund, Grant for Research: Government Budget, Chulalongkorn University (2018), and the National Research Council of Thailand (NRCT) for their financial support of this project.

References

[1] A. Paul, R. S. Panua, D. Debroy, and P. K. Bose, "Effect of diethyl ether and ethanol on performance, combustion, and emission of single-cylinder compression ignition engine," *International Journal of Ambient Energy*, vol. 38, no. 1, pp. 2–13, 2014.

[2] M. R. Mostafa, A. M. Youssef, and S. M. Hassan, "Conversion of ethanol and isopropanol on alumina, titaniaand alumina-titania catalysts," *Materials Letters*, vol. 12, no. 3, pp. 207–213, 1999.

[3] H. Nair, J. E. Gatt, J. T. Miller, and C. D. Baertsch, "Mechanistic insights into the formation of acetaldehyde and diethyl ether from ethanol over supported VO*x*, MoO*x*, and WO*x* catalysts," *Journal of Catalysis*, vol. 279, no. 1, pp. 144–154, 2011.

[4] T. Zaki, "Catalytic dehydration of ethanol using transition metal oxide catalysts," *Journal of Colloid and Interface Science*, vol. 284, no. 2, pp. 606–613, 2005.

[5] Y. Xiao, X. Li, Z. Yuan, J. Li, and Y. Chen, "Catalytic dehydration of ethanol to ethylene on TiO_2/4A zeolite composite catalysts," *Catalysis Letters*, vol. 130, no. 3-4, pp. 308–311, 2009.

[6] I. Rossetti, M. Compagnoni, E. Finocchio et al., "Ethylene production via catalytic dehydration of diluted bioethanol: a step towards an integrated biorefinery," *Applied Catalysis B: Environmental*, vol. 210, pp. 407–420, 2017.

[7] T. K. Phung and G. Busca, "Ethanol dehydration on silica-aluminas: active sites and ethylene/diethyl ether selectivities," *Catalysis Communications*, vol. 68, pp. 110–115, 2015.

[8] A. Popa and V. Sasca, "The influence of surface coverage on the catalytic activity of silica-supported heteropolyacids," *Reaction Kinetics, Mechanisms and Catalysis*, vol. 117, no. 1, pp. 205–221, 2015.

[9] S. Bagheri, N. Muhd Julkapli, and S. Bee Abd Hamid, "Titanium dioxide as a catalyst support in heterogeneous catalysis," *Scientific World Journal*, vol. 2014, Article ID 727496, 21 pages, 2014.

[10] M. Dalil, D. Carnevali, J.-L. Dubois, and G. S. Patience, "Transient acrolein selectivity and carbon deposition study of glycerol dehydration over WO_3/TiO_2 catalyst," *Chemical Engineering Journal*, vol. 270, pp. 557–563, 2015.

[11] U. Filek, A. Kirpsza, A. Micek-Ilnicka, E. Lalik, and A. Bielański, "Ethanol conversion over cesium-doped mono- and bi-cationic aluminum and gallium H3PW12O40 salts," *Journal of Molecular Catalysis A: Chemical*, vol. 407, pp. 152–162, 2015.

[12] D. T. Mai, I. I. Mikhalenko, and A. I. Pylinina, "Hydrothermal ethanol conversion on Ag, Cu, Au/TiO_2," *Russian Journal of Physical Chemistry A*, vol. 88, no. 10, pp. 1637–1642, 2014.

[13] G. Pérez-López, R. Ramírez-López, and T. Viveros, "Acidic properties of Si- and Al- promoted TiO_2 catalysts: effect on 2-propanol dehydration activity," *Catalysis Today*, vol. 305, pp. 182–191, 2018.

[14] T. Kamsuwan, P. Praserthdam, and B. Jongsomjit, "Diethyl ether production during catalytic dehydration of ethanol over Ru- and Pt- modified H-beta zeolite catalysts," *Journal of Oleo Science*, vol. 66, no. 2, pp. 199–207, 2017.

[15] M. Sudhakar, V. V. Kumar, G. Naresh, M. L. Kantam, S. K. Bhargava, and A. Venugopal, "Vapor phase hydrogenation of aqueous levulinic acid over hydroxyapatite supported metal (M = Pd, Pt, Ru, Cu, Ni) catalysts," *Applied Catalysis B: Environmental*, vol. 180, pp. 113–120, 2016.

[16] T. Inmanee, P. Pinthong, and B. Jongsomjit, "Effect of calcination temperatures and Mo modification on nanocrystalline (γ-χ)-Al_2O_3 catalysts for catalytic ethanol dehydration," *Journal of Nanomaterials*, vol. 2017, pp. 1–9, 2017.

[17] J. Chauvin, K. Thomas, G. Clet, and M. Houalla, "Comparative influence of surface tungstate species and bulk amorphous WO_3 particles on the acidity and catalytic activity of tungsten oxide supported on silica," *Journal of Physical Chemistry C*, vol. 119, no. 22, pp. 12345–12355, 2015.

[18] P. Lauriol-Garbey, S. Loridant, V. Bellière-Baca, P. Rey, and J.-M. M. Millet, "Gas phase dehydration of glycerol to acrolein over WO_3/ZrO_2 catalysts: improvement of selectivity and stability by doping with SiO_2," *Catalysis Communications*, vol. 16, no. 1, pp. 170–174, 2011.

[19] J. A. Cecilia, C. García-Sancho, J. M. Mérida-Robles, J. Santamaría González, R. Moreno-Tost, and P. Maireles-Torres, "WO_3 supported on Zr doped mesoporous SBA-15 silica for glycerol dehydration to acrolein," *Applied Catalysis A: General*, vol. 516, pp. 30–40, 2016.

[20] M. Ai, "The activity of WO_3-based mixed-oxide catalysts: I. Acidic properties of WO_3-based catalysts and correlation with catalytic activity," *Journal of Catalysis*, vol. 49, no. 3, pp. 305–312, 1977.

[21] V. Lebarbier, G. Clet, and M. Houalla, "Relations between structure, acidity, and activity of WO_x/TiO_2: influence of the initial state of the support, titanium oxyhydroxide, or titanium oxide," *Journal of Physical Chemistry B*, vol. 110, no. 45, pp. 22608–22617, 2006.

[22] Y. Qin, S. Xun, L. Zhan et al., "Synthesis of mesoporous WO_3/TiO_2 catalyst and its excellent catalytic performance for the oxidation of dibenzothiophene," *New Journal of Chemistry*, vol. 41, no. 2, pp. 569–578, 2017.

[23] X. Zhao, L. Mao, and G. Dong, "Mn-Ce-V-WO_x/TiO_2 SCR catalysts: catalytic activity, stability and interaction among catalytic oxides," *Catalysts*, vol. 8, no. 2, p. 76, 2018.

[24] C. Liebig, S. Paul, B. Katryniok et al., "Glycerol conversion to acrylonitrile by consecutive dehydration over WO_3/TiO_2 and

ammoxidation over Sb-(Fe, V)-O," *Applied Catalysis B: Environmental*, vol. 132-133, pp. 170–182, 2013.

[25] Y. M. Hunge, M. A. Mahadik, A. V. Moholkar, and C. H. Bhosale, "Photoelectrocatalytic degradation of oxalic acid using WO_3 and stratified WO_3/TiO_2 photocatalysts under sunlight illumination," *Ultrasonics Sonochemistry*, vol. 35, pp. 233–242, 2017.

[26] T. K. Phung, L. Proietti Hernández, and G. Busca, "Conversion of ethanol over transition metal oxide catalysts: effect of tungsta addition on catalytic behaviour of titania and zirconia," *Applied Catalysis A: General*, vol. 489, pp. 180–187, 2015.

[27] H. V. Fajardo, E. Longo, E. R. Leite, R. Libanori, L. F. D. Probst, and N. L. V. Carreño, "Synthesis, characterization and catalytic properties of nanocrystaline $Y2O_3$-coated TiO_2 in the ethanol dehydration reaction," *Materials Research*, vol. 15, no. 2, pp. 285–290, 2012.

[28] M. Wannaborworn, P. Praserthdam, and B. Jongsomjit, "A comparative study of solvothermal and sol-gel-derived nanocrystalline alumina catalysts for ethanol dehydration," *Journal of Nanomaterials*, vol. 2015, Article ID 519425, 11 pages, 2015.

[29] J. Panpranot, K. Kontapakdee, and P. Praserthdam, "Selective hydrogenation of acetylene in excess ethylene on micron-sized and nanocrystalline TiO_2 supported Pd catalysts," *Applied Catalysis A: General*, vol. 314, no. 1, pp. 128–133, 2006.

[30] C. M. Gómez-Gutiérrez, P. A. Luque, G. Guerra-Rivas et al., "Solvothermal synthesis of nickel-tungsten sulfides for 2-propanol dehydration," *Scanning*, vol. 37, no. 3, pp. 165–171, 2015.

[31] C. Krutpijit and B. Jongsomjit, "Catalytic ethanol dehydration over different acid-activated montmorillonite clays," *Journal of Oleo Science*, vol. 65, no. 4, pp. 347–355, 2016.

[32] K. Thamaphat, P. Limsuwan, and B. Ngotawornchai, "Phase characterization of TiO_2 powder by XRD and TEM," *Natural Science*, vol. 42, pp. 357–361, 2008.

[33] B. S. Shirke, P. V. Korake, P. P. Hankare, S. R. Bamane, and K. M. Garadkar, "Synthesis and characterization of pure anatase TiO_2 nanoparticles," *Journal of Materials Science: Materials in Electronics*, vol. 22, no. 7, pp. 821–824, 2010.

[34] A. A. Said, M. M. M. Abd El-Wahab, and M. Abd El-Aal, "The role of acid sites in the catalytic performance of tungsten oxide during the dehydration of isopropyl and methyl alcohols," *Chemical and Materials Engineering*, vol. 4, no. 2, pp. 17–25, 2016.

[35] S. Maksasithorn, P. Praserthdam, K. Suriye, and D. P. Debecker, "Preparation of super-microporous WO_3-SiO_2 olefin metathesis catalysts by the aerosol-assisted sol-gel process," *Microporous and Mesoporous Materials*, vol. 213, pp. 125–133, 2015.

[36] R. E. M. Abdennouri, A. Elmhammedi, A. Galadi et al., "Influence of tungsten on the anatase-rutile phase transition of sol-gel synthesized TiO_2 and on its activity in the photocatalytic degradation of pesticides," *Journal of Materials and Environmental Science*, vol. 4, no. 6, pp. 953–960, 2013.

[37] M. Almohalla, I. Rodríguez-Ramos, and A. Guerrero-Ruiz, "Comparative study of three heteropolyacids supported on carbon materials as catalysts for ethylene production from bioethanol," *Catalysis Science & Technology*, vol. 7, no. 9, pp. 1892–1901, 2017.

[38] T. Kamsuwan and B. Jongsomjit, "A comparative study of different Al-based solid acid catalysts for catalytic dehydration of ethanol," *Engineering Journal*, vol. 20, no. 3, pp. 63–75, 2016.

[39] H. Xin, X. Li, Y. Fang et al., "Catalytic dehydration of ethanol over post-treated ZSM-5 zeolites," *Journal of Catalysis*, vol. 312, pp. 204–215, 2014.

[40] K.-M. C. David Raju Burri, S.-C. Han, A. Burri, and S.-E. Park, "Dehydrogenation of ethylbenzene to styrene with CO_2 over TiO_2-ZrO_2 bifunctional catalyst," *Bulletin of the Korean Chemical Society*, vol. 28, no. 1, pp. 53–58, 2007.

[41] D. Chen, D. Mao, J. Xiao, X. Guo, and J. Yu, "CO_2 hydrogenation to methanol over CuO-ZnO-TiO_2-ZrO_2: a comparison of catalysts prepared by sol-gel, solid-state reaction and solution-combustion," *Journal of Sol-Gel Science and Technology*, vol. 86, no. 3, pp. 719–730, 2018.

[42] S. L. Chong, J. C. Soh, and C. K. Cheng, "Production of ethylene from ethanol dehydration over H_3PO_4- modified cerium oxide catalyst," *Malaysian Journal of Analytical Sciences*, vol. 21, no. 4, pp. 839–848, 2017.

[43] W. Alharbi, E. Brown, E. F. Kozhevnikova, and I. V. Kozhevnikov, "Dehydration of ethanol over heteropoly acid catalysts in the gas phase," *Journal of Catalysis*, vol. 319, pp. 174–181, 2014.

[44] E. Hong, H.-I. Sim, and C.-H. Shin, "The effect of Brønsted acidity of WO_3/ZrO_2 catalysts in dehydration reactions of C_3 and C_4 alcohols," *Chemical Engineering Journal*, vol. 292, pp. 156–162, 2016.

[45] W. R. Moser, R. W. Thompson, C.-C. Chang, and H. Tong, "Silicon-rich H-ZSM-5 catalyzed conversion of aqueous ethanol to ethylene," *Journal of Catalysis*, vol. 117, no. 1, pp. 19–32, 1989.

[46] C. P. Nash, A. Ramanathan, D. A. Ruddy et al., "Mixed alcohol dehydration over Brønsted and Lewis acidic catalysts," *Applied Catalysis A: General*, vol. 510, pp. 110–124, 2016.

[47] C. Autthanit and B. Jongsomjit, "Production of ethylene through ethanol dehydration on SBA-15 catalysts synthesized by sol-gel and one-step hydrothermal methods," *Journal of Oleo Science*, vol. 67, no. 2, pp. 235–243, 2018.

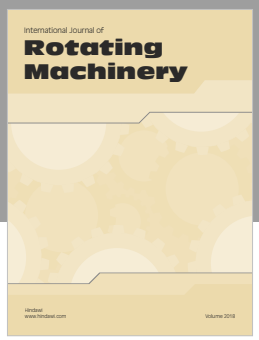

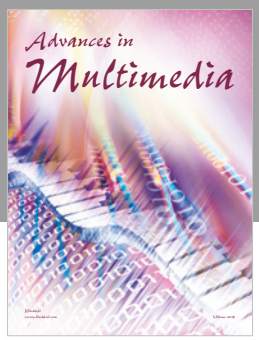

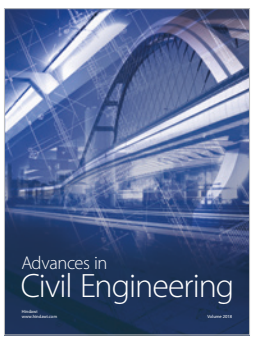

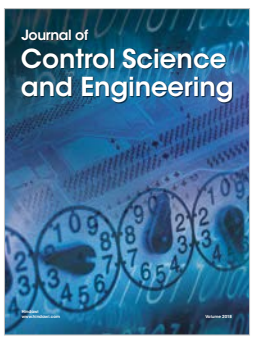

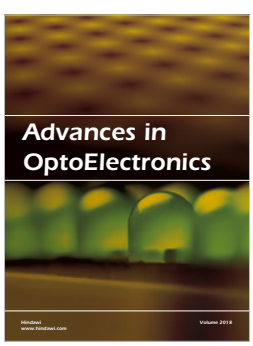

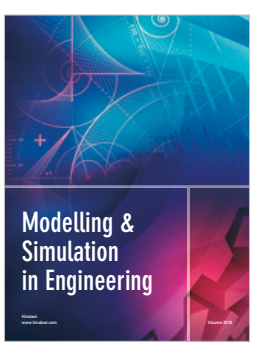

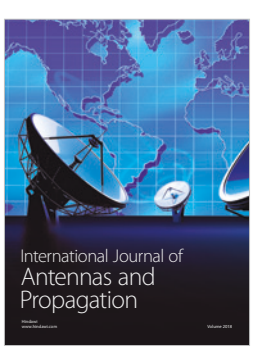

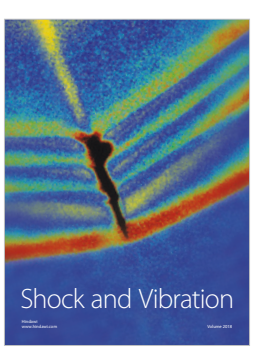

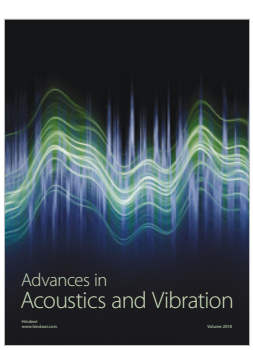

Hindawi

Submit your manuscripts at
www.hindawi.com